The following publication M. Chen et al., "An Advanced Integrated Sensor-Based Method for Fall Risk Assessment in Rehabilitation Setting," in IEEE Sensors Journal, vol. 25, no. 8, pp. 13685-13695, 15 April, 2025 is available at https://doi.org/10.1109/JSEN.2025.3547925.

An advanced integrated sensor-based method for fall risk assessment in rehabilitation setting

Manting Chen, Lu Zhang, Lisha Yu, Eric Hiu Kwong Yeung, Qizheng Zhao, Junjie Cao, Xuan Wang, Jiacheng Huang, Hailiang Wang*, and Yang Zhao*

***Abstract*— Falls are the most common preventable adverse events in hospitals and are strongly linked to movement-related disorders. Conducting fall risk assessments and implementing personalized interventions for older adults in sport rehabilitation settings can significantly reduce fall incidence. Sensor-based techniques and machine learning models offer new opportunities for measuring gait and balance in a more sophisticated way to enhance fall risk assessments. This study aims to develop an integrated sensor method to provide continuous and effective fall risk assessments for older adults in rehabilitation settings. A joint feature extraction scheme based on integrated sensors was proposed, including temporal features from inertial measurement unit signals and spatial features from depth camera data during 3–meter Timed Up and Go test. A set of classifiers, including Support Vector Machine, Logistic Regression, K-Nearest Neighbors, Random Forest, and XGBoost, in conjunction with feature selection strategy was employed to facilitate developing the predictive models for fall risk assessment. We conducted validation experiments using real-world data for comprehensive comparative analysis. The result demonstrates that our integrated approach achieves superior classification performance (AUC: 0.8633–0.9586). These findings suggest that the complementary features from sensors have advantages in bridging information gaps, reducing missed diagnoses, and assisting clinicians in early fall risk identification. The proposed method shows significant potential to deliver comprehensive fall risk assessments for older adults in rehabilitation settings.**

***Index Terms*— fall risk assessment, rehabilitation, inertial measurement units, depth camera, gait and balance parameters.**

This research was funded by the National Key Research and Development Program of China, grant number 2023YFC2307305, the Shen Zhen–Hong Kong–Macao Science and Technology Project Fund, grant number SGDX20210823103403028, the Joint Postdoc Scheme with Non-local Institutions, grant number P0042959, and the School Awards for Outstanding Achievement, grant number P0045769 at the Hong Kong Polytechnic University. (*Corresponding author: Yang Zhao and Hailiang Wang)

Manting Chen and Lu Zhang contributed equally to this research work.
Manting Chen, Lu Zhang, Qizheng Zhao, Junjie Cao, Xuan Wang, and Yang Zhao* are with Intelligent Sensing and Proactive Health Research Center, School of Public Health (Shenzhen), Sun Yat-sen University, Shenzhen 518000, China (e-mail: mantingchen1998@gmail.com; zhanglu69@mail2.sysu.edu.cn; zhaoqzh@mail2.sysu.edu.cn; caojj28@mail2.sysu.edu.cn; wangx789@mail2.sysu.edu.cn; zhaoy393@mail.sysu.edu.cn).
Lisha Yu is with the School of data science, Lingnan university, Hong Kong 999077, China (e-mail: lishayu@ln.edu.hk)
Hailiang Wang is with the School of Design, The Hong Kong Polytechnic University, Hung Hom, Hong Kong 999077, China (e-mail: hailiang.wang@polyu.edu.hk).
Eric Hiu Kwong Yeung and Jiacheng Huang are with the Department of Physiotherapy, The University of Hong Kong-Shenzhen Hospital, Shenzhen 518000, China (e-mail: yangxg@hku-szh.org; huangjc@hku-szh.org).

I. Introduction

FALLS are among the most frequently reported preventable adverse events in hospitals [1], with incidence rates in Chinese hospitals ranging from 1.4‰ to 18.2‰ [2]. They are strongly linked to movement-related disorders, including cerebrovascular disease, neurological conditions (e.g., Parkinson's syndrome), musculoskeletal disorders (e.g., joint replacement, osteoarthritis), and pain-related conditions (e.g., lumbar disc herniation, muscle and tendon injuries) [3]. Older adults exhibit a high prevalence of cerebrovascular diseases [4] and face increased risks of sarcopenia and bone calcium loss [5]. They constitute a substantial proportion of patients in rehabilitation departments [6] and are at high risk for inpatient falls [2]. Inpatient wards in sports rehabilitation departments often manage patients with multiple movement-related disorders and a high proportion of older adults. Implementing fall risk assessments and tailored interventions have significantly reduced fall incidence among older adults in healthcare settings [4], [6], [7].

Some studies rely on epidemiological survey data to assess fall risk [8]; however, such data are often outdated and fail to capture dynamic changes, limiting their suitability for evaluating patients during rehabilitation. Other studies employ standardized functional tests, such as the widely used 3-meter Timed Up and Go (TUG) test [9], to classify fall risk levels based on completion time. Although the TUG test is simple and highly practical, its broad time thresholds fail to provide detailed insights into muscle strength, balance, and mobility, limiting its interpretability and clinical utility. Despite the widespread adoption of the 13.5-second criterion in many studies [10], no universally accepted standard currently exists. For instance, a review by Beauchet et al. [11] summarized TUG time thresholds across various aging populations, reporting values ranging from 10 to 32.6 seconds.

The Berg Balance Scale (BBS) is widely regarded as the gold standard for fall risk screening [12]. It offers detailed scoring criteria with high interpretability and has demonstrated reliable accuracy in assessing fall risk in both communities [13] and institutional settings [14]. Hospitalized older patients

in rehabilitation departments often exhibit significant mobility impairments, necessitating frequent clinical assessments to reduce fall risk. A single BBS assessment in community-dwelling older adults typically requires 10-20 minutes, with potentially longer durations for hospitalized patients, placing substantial demands on healthcare resources. The TUG test and BBS have shown strong consistency in their results [15], [16]. Therefore, we propose integrating the simplicity of the 3M-TUG with the accuracy of the BBS to develop a low-cost, efficient, and automated fall risk assessment method tailored to geriatric patients in rehabilitation settings.

Sensor-based techniques have gained increasing attention in fall risk assessment [17], with inertial measurement units (IMUs) and depth cameras being the two most prominent devices in this field. IMUs, which integrate accelerometers and gyroscopes, are widely recognized for their motion monitoring capabilities and wearability [18]. Statistical features of IMU data (e.g., standard deviation, skewness), as well as frequency features (e.g., peak frequency, spectral frequency), and time-frequency features, have shown effectiveness in predicting fall risk [19]. Kinect v2, a markerless device, captures 3D body motion in real time using an RGB-D sensor that integrates a color (RGB) camera and a depth (D) sensor. Kim et al. [20] and Latorre et al. [21] extracted spatiotemporal and kinematic gait features from the 3M-TUG test, including gait speed, stride length and step duration, reporting AUC values of 84.7% and 86.6%, respectively.

Although IMUs and depth cameras have demonstrated acceptable measurement accuracy [22], [23] in older adults, including those in community settings or with specific diseases, their reliability in complex rehabilitation environments remains uncertain. Kinect's depth capture is highly sensitive to environmental factors [24], [25] and demonstrates reduced accuracy for small anterior-posterior movements [26], whereas IMUs are susceptible to sensor drift [27]. Given the high accuracy of IMUs in capturing subtle human motions and the capabilities of Kinect in advanced gait analysis, it is worth exploring the potential integration of depth cameras and IMUs into a unified fall risk analysis method. Some studies have demonstrated the efficacy of integrating IMUs and depth cameras for various research applications [28]–[30]. However, the use of this integrated approach for screening specific rehabilitation needs remains underexplored.

In this study, we developed an effective and easy-to-implement fall risk screening approach for older adults in rehabilitation settings, where multiple movement-related disorders often coexist. Specifically, we investigated the complementary effects between IMU signals and depth camera data collected from individual functional tests, enabling timely and accurate gait measurements with less reliance on healthcare professionals in rehabilitation progress. A joint feature extraction scheme based on integrated sensors was developed, including both temporal and spatial features. Through feature selection and machine learning models, we identified the key features relevant to fall risk in geriatric patients and validated the integrated approach's performance via field study in a local hospital. The result demonstrates that our integrated approach achieves superior performance on fall risk assessment. Overall, this study aims to enhance fall risk screening capabilities for geriatric patients, promote transparency in medical decision-making, prevent inpatient falls, optimize medical utilization resources, and improve healthcare efficiency.

The remainder of this paper is organized as follows. Section 2 describes the study design, data collection, sensor setup, and feature engineering methods. Section 3 introduces the machine learning models utilized in this study. Section 4 presents key motor features and evaluates the predictive performance of the models. Section 5 discusses the complementary effects of the sensors, the physiological interpretation of features, the practical feasibility of the integrated method in rehabilitation scenarios, and the discrepancy between BBS and TUG.

II. Materials and Methods

A. Schematic Diagram

Figure 1 illustrates an interpretable fall risk assessment method specifically designed for geriatric patients with movement-impairing conditions in rehabilitation. This method captures and records essential health-related information, such as gait patterns and motion status, generated through the 3M-TUG test. Advanced data mining techniques are employed to integrate and analyze the data obtained from wearable sensors and a depth camera via a computer where an algorithm assesses the subject's fall risk. Based on the fall risk level determined by the algorithm, along with self-reported health conditions and objective demographic information, therapists can leverage their expertise to provide comprehensive and detailed intervention recommendations. Patients and their families receive these personalized and transparent medical decisions, which enhances their confidence in treatment and improves rehabilitation outcomes.

This work integrates IMU and Kinect devices, enhancing the interpretability and classification capability of fall risk assessment. It provides personalized guidance for individual rehabilitation while also facilitating the efficient management of healthcare resources.

B. Experiment Protocol

Falls are primarily the result of aging processes affecting both the sensorimotor and cognitive domains [31], leading to deterioration in the structural and functional integrity of the central nervous system, peripheral sensory receptors, and the musculoskeletal system. Among geriatric rehabilitation patients, aging may serve as a risk factor for common conditions such as neurological disorders and musculoskeletal injuries, while aging and these conditions together contribute to the occurrence of fall events. Falls in older rehabilitation patients are associated with lower extremity strength, transitional movements, balance [32], and proprioception [33], with this decline characterized by impaired balance control, altered gait patterns, and reduced mobility [34].

We utilized the 3M-TUG test to evaluate subjects' gait mobility, lower extremity strength, proprioception, and transitional movements. Additionally, registered physiotherapists used the Berg Balance Scale (BBS) to identify fall-prone individuals, with a BBS score of ≤ 40 indicating high fall risk.

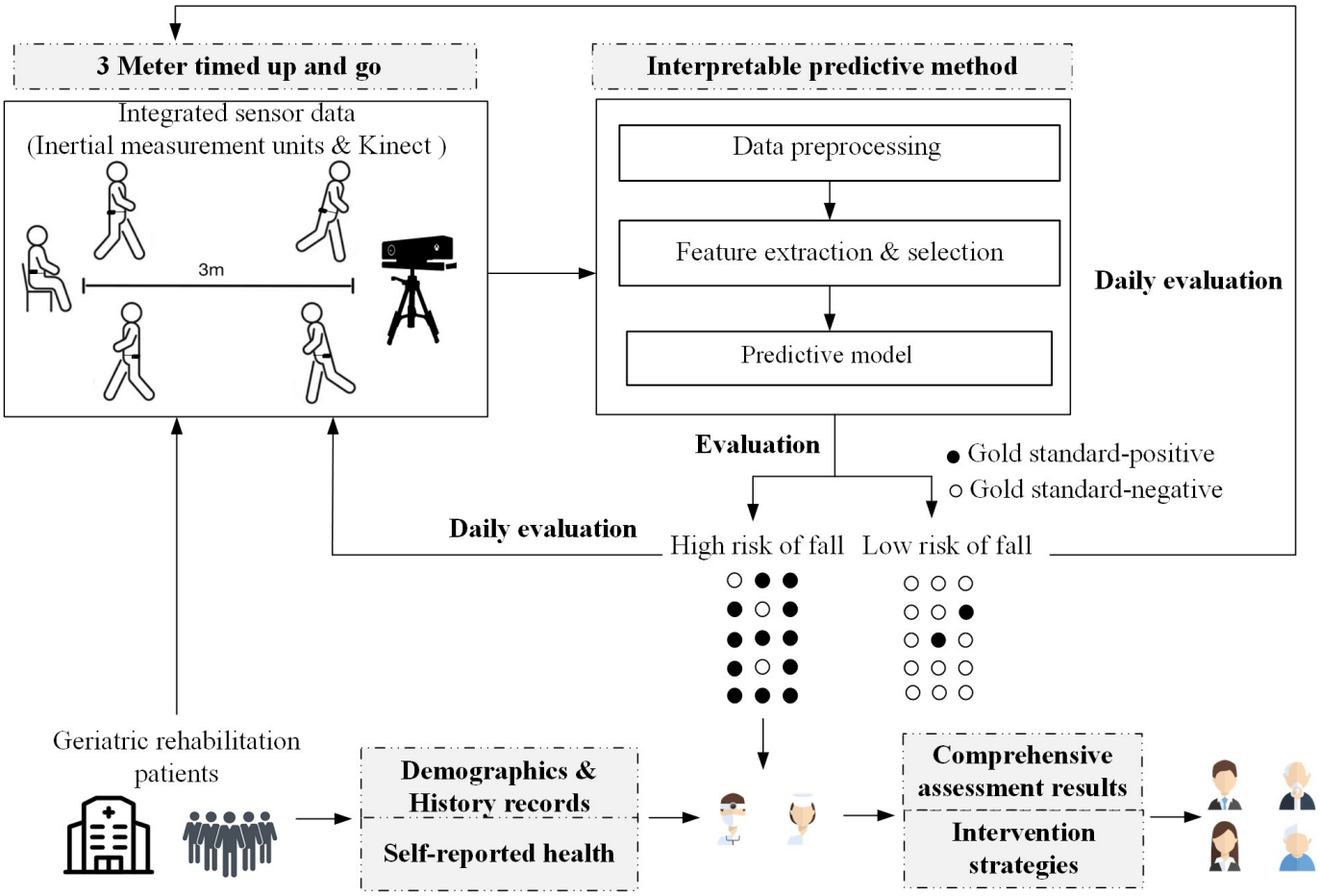

Fig. 1 Schematic Diagram of the Proposed Fall-risk-assessment Method

To further enhance the performance of the fall risk assessment method, we integrated a depth camera and IMUs into the evaluation process.

1) 3-meter Timed Up and Go (3M-TUG): In the 3M-TUG test, the patient is asked to stand up from a chair, walk for 3 meters, turn, walk back to the chair, and sit down; it typically takes less than 13.5 seconds to complete at comfortable gait speed in healthy older people and is used to assess gait mobility [10]. In this study, the participants wore an IMU (consisting primarily of an accelerometer and a gyroscope) before performing the 3M-TUG test. The sensor data of the 3M-TUG test was recorded as it is associated with impaired mobility and increased fall risks.

2) Berg Balance Scale (BBS): The Berg Balance Scale consists of 14 items, each scored on a five-level scale ranging from 0 to 4 points, with a maximum total score of 56 points. For specific items, see Table I. The final score is obtained by summing the scores of all items, which reflects the overall balance ability of the individual being assessed. Higher scores indicate better balance ability.

TABLE I ITEMS OF THE BERG BALANCE SCALE

Item Number	Mobility Task
1	Sitting to standing
2	Standing unsupported
3	Sitting unsupported
4	Standing to sitting
5	Transfers
6	Standing with eyes closed
7	Standing with feet together
8	Reaching forward with outstretched arm
9	Picking up an object from the floor
10	Turning to look behind
11	Turning 360 degrees
12	Placing alternate foot on step or stool
13	Standing with one foot in front
14	Standing on one foot

3) Hardware Setup: The devices used in our method include a computer, inertial measurement units (IMUs), and Kinect 2.0. IMUs is a 9-axis sensor that measures orientation, velocity, and gravitational forces by combining an accelerometer, gyroscope, and magnetometer. With advancements in Micro Electromechanical System (MEMS) technology, IMUs are now typically miniaturized sensors designed for easy integration with microcontrollers. The IMU used in this study had

a sampling frequency of 100 Hz and was placed on the L4 vertebrae (Figure 2) of participants, which is also considered the most commonly used placement location [31]. This study utilized only the acceleration and angular velocity data collected from the accelerometer and gyroscope for analysis.

Kinect 2.0 is a motion-sensing interactive device developed by Microsoft. It consists of an infrared (IR) projector, an IR camera, an RGB camera, and a multi-array microphone. When the skeletal data stream of the Kinect sensor is activated, it can rapidly detect a human body within its field of vision and track skeletal movements in real time. Kinect 2.0 provides a 25-joint skeletal model with three-dimensional coordinates, allowing the motion of each body part to be analyzed individually. In this study, a Kinect sensor was positioned 4.16 m from the participant's chair to capture movement data from all 25 joints.

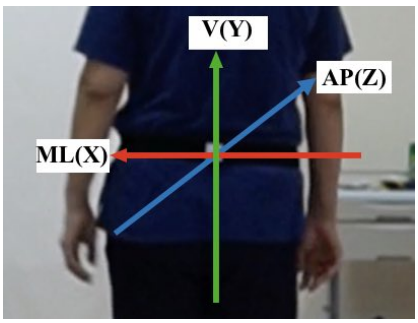

Fig. 2 Illustration of the Direction of IMU

C. Data Collection

1) Participants: In our experimental study, we recruited older adults who met the following inclusion criteria:

a) Expected that the patient would be able to participate in a rehabilitation program for more than one week.
b) At least 60 years old.
c) Willing to participate in the study.
d) Capable of cooperating in the assessment.

Participants with unstable or life-threatening illnesses, physical injuries, or health conditions that impacted independent walking were excluded from the study. The pilot study was approved by the Research Ethics Committees of the affiliated university and the collaborating hospital and was registered on the Chinese Clinical Trial Registry (ChiCTR) with approval number ChiCTR2200061834. All of the participants had provided written informed consent before participating in the study.

2) Procedure: The implementation phase was scheduled in the Department of Rehabilitation at a local hospital from July 20, 2022, to October 26, 2022. A total of 56 participants were recruited, and 31 completed both the questionnaire and the test.

After obtaining the participants' consent forms, customized questionnaires were used to collect the older adults' demographic information (e.g., age, sex, living status, medication, history of smoking and alcohol consumption, and chronic disease history). Next, the IMU sensor was attached to the participants' lumbar spine (L4). Meanwhile, the Kinect sensor was activated to begin signal collection. After receiving detailed instructions on the test procedures, the participants performed the 3M-TUG test once, followed by a professional physiotherapist assessing their BBS performance.

D. Data Preprocessing

In this study, a fourth-order Butterworth filter with a cutoff frequency of 10 Hz was applied to denoise the raw IMU data. For the Kinect skeletal data, mean filtering (window size of 15) and Gaussian filtering (with a Gaussian kernel size of 15 and a standard deviation of 5) were first used to remove noise, followed by a Savitzky-Golay filter (window size of 15, polyorder of 3) for signal smoothing.

Additionally, a significant aspect of our data preprocessing involved calculating the ankle differential during the 3M-TUG task, utilizing data from the Kinect sensor. Defined by the equation Ankle diff = Left anklez - Right anklez, this differential measures the variance between the z-axis positions of the left and right ankles. We calculated this metric on the 3M-TUG time series and used a threshold algorithm for subtask segmentation, facilitating subsequent feature extraction.

E. Feature Extraction and Selection

To identify significant predictive features in the complex scenario of comorbid diseases in rehabilitation settings, we integrated IMU and Kinect features highlighted in previous studies. These features have been recognized for their excellent predictive ability in populations such as low functional community-dwelling older adults [30], individuals with neurological disorders, and patients with musculoskeletal diseases [35].

For IMU data, we extracted statistical parameters, such as extreme values, means, and root mean square (RMS); higher-order statistics, including kurtosis and skewness; and nonlinear features, such as Shannon entropy, for the three-axis acceleration and three-axis angular velocity, as well as the acceleration and angular velocity vectors. Additionally, frequency domain features, such as spectral energy and spectral peak, were extracted specifically for the acceleration and angular velocity vectors.

For Kinect data, we derived spatiotemporal parameters during walking (by merging the two walking segments before and after turning), such as step count, average step length, average step width, and gait speed, as well as the average curvature during turning. It is worth noting that the segmentation of 3M-TUG subtasks primarily aimed to separately extract spatiotemporal features for walking and turning, as well as temporal features for each subtask, which were derived from Kinect data. In contrast, IMU features were calculated for the entire task as a whole. A complete list of extracted features is provided in Table II and III.

To mitigate dimensionality and reduce the risk of overfitting, we first conducted statistical tests to select features with significant inter-group differences ($p < 0.05$). This study implemented sensor integration at the feature level, first selecting the eight most important features respectively from

the IMU and Kinect datasets using the Boruta method, and then combining them into an integrated sensor feature set. The Boruta method, based on random forest, evaluates the importance of each real feature by comparing it with randomly shuffled "shadow features". This iterative process discards non-informative features while retaining those with substantial predictive relevance.

TABLE II SUMMARY OF FEATURES EXTRACTED FROM KINECT IN 3M-TUG

Device	Subtask	Feature name	Unit
Kinect	Sit to stand	Chair rise time	s
	Stand to sit	Chair descent time	s
	Walking	Walking time	s
		Step count	-
		Mean stride length	m
		Mean step length	m
		Mean step width	m
		Cadence	steps/min
		Walk speed	m/s
	Turning	Turning time	s
		Average path curvature	1/m
		Turning width	m
	Overall	Total time	s

TABLE III SUMMARY OF FEATURES EXTRACTED FROM IMU IN 3M-TUG

Device	Feature name	Unit	Direction
IMU	Maximum value	m/s^2	V, AP, ML
	Minimum value	m/s^2	V, AP, ML, Magnitude
	Range	m/s^2	V, AP, ML, Magnitude
	Mean value	m/s^2	V, AP, ML, Magnitude
	Root mean square	m/s^2	V, AP, ML, Magnitude
	Standard deviation	m/s^2	V, AP, ML, Magnitude
	Mean jerk	m/s^3	V, AP, ML, Magnitude
	Coefficient of variation	-	V, AP, ML, Magnitude
	Shannon entropy	-	V, AP, ML, Magnitude
	Sample entropy	-	V, AP, ML, Magnitude
	Kurtosis	-	V, AP, ML, Magnitude
	Skewness	-	V, AP, ML, Magnitude
	Spectral centroid	-	Magnitude
	Spectral energy	-	Magnitude
	Spectral entropy	-	Magnitude
	Spectral peak	-	Magnitude
	Spectral bandwidth	-	Magnitude

Note: V = vertical direction, AP = anteroposterior direction, ML = mediolateral direction, Magnitude is calculated as:

$$\text{Magnitude} = \sqrt{V^2 + AP^2 + ML^2}$$

III. Predictive Model

A. Support Vector Machine (SVM)

Support Vector Machine can serve as a binary classification model designed to find an optimal hyperplane that separates data from different classes while maximizing the margin between them. This hyperplane is defined by the equation $w \cdot x + b = 0$. The geometric margin for a sample point (x_i, y_i) relative to this hyperplane is given by:

$$\gamma_i = \frac{y_i(\mathbf{w} \cdot \mathbf{x}_i + b)}{|\mathbf{w}|} \tag{1}$$

Where $\mathbf{w}$ is the hyperplane's normal vector, determining the direction of the classification boundary. b is bias term, adjusting the position of the classification boundary. $\mathbf{x}_i$ is the feature vector of the ith sample. y_i is class label of the sample, taking values of $\{+1, -1\}$ that corresponds to high and low fall risk, respectively. $\|\mathbf{w}\|$ is the norm of vector $\mathbf{w}$, used for normalization.

The minimum margin across all samples is calculated as:

$$\gamma = \min_{i=1,2,\ldots,N} \gamma_i \tag{2}$$

SVMs are particularly efficient in model training because only the support vectors, which are the samples on the margin boundaries, are crucial for determining the final model. This property reduces the complexity and improves the generalization ability of the model.

B. Logistic Regression (LR)

Logistic regression is a generalized linear model used for classification tasks. The model uses the sigmoid function (3) to map the output of linear regression into probability values, which are compared to a predefined probability threshold to predict the likelihood of belonging to a specific class. Logistic regression typically employs the cross-entropy loss function (4), where a smaller loss indicates better classification performance of the model.

$$\sigma(x_i) = \frac{1}{1 + e^{-x_i}} \tag{3}$$

The cross-entropy loss function is defined as:

$$\begin{aligned} J(\beta) &= -\log L(\beta) \\ &= -\sum_{i=1}^{n} \big[y_i \log P(y_i) \\ &\quad + (1 - y_i) \log(1 - P(y_i)) \big] \end{aligned} \tag{4}$$

Where $J(\beta)$ is the Loss function value to be minimized. y_i is the actual class label for the i-th sample, and $P(y_i)$ is the predicted probability of the i-th sample belonging to its actual class.

C. K-Nearest Neighbors (KNN)

K-Nearest Neighbors is an instance-based algorithm. In this learning technique, the training phase involves simply storing the samples, resulting in zero training time overhead. The classification result for a test sample is determined by the

majority class among the k-nearest neighbors in the training set. Based on a given distance metric, the k-nearest points to x in the training set T are identified.

The neighborhood of x, denoted as $\mathcal{N}_k(x)$, contains these k points. The class y of x is determined according to a classification decision rule (e.g., majority voting) within $\mathcal{N}_k(x)$, where I in Equation (5) represents the indicator function. The feature space for KNN is typically an n-dimensional real vector space $\mathcal{R}_n$, and the distance metric used is commonly the L_p-norm, with the most typical choice being the Euclidean distance (6).

$$y = \arg\max_{c_j} \sum_{x_i \in \mathcal{N}_k(x)} I(y_i = c_j), \tag{5}$$

$$\begin{aligned} L_p(x_i, x_j) &= \left(\sum_{l=1}^{n} \left| x_i^{(l)} - x_j^{(l)} \right|^p \right)^{\frac{1}{p}} \\ i &= 1, 2, \ldots, N; \\ j &= 1, 2, \ldots, K \end{aligned} \tag{6}$$

Where $\mathcal{N}_k(x)$ is the neighborhood of x containing k nearest points. $L_p(x_i, x_j)$ is the distance metric between points x_i and x_j. $I(y_i = c_j)$ is the indicator function, equaling to 1 if $y_i = c_j$ otherwise 0.

D. Random Forest (RF)

Random Forest is a Bagging algorithm that uses decision trees as estimators. For each iteration, a random subset of the dataset is selected with replacement, and a random subset of features is chosen as input for training.

CART decision trees in the random forest algorithm split the data based on the Gini index (7). The attribute that results in the greatest reduction in the Gini index after splitting is selected as the splitting attribute.

$$Gini(D) = \sum_{k=1}^{n} \sum_{k' \neq k} p_k p_{k'} = 1 - \sum_{k=1}^{n} p_k^2 \tag{7}$$

Where $Gini(D)$ is the Gini index of dataset D, measuring impurity, and p_k is the proportion of samples in class k.

E. eXtreme Gradient Boosting (XGBoost)

XGBoost, short for eXtreme Gradient Boosting, is a type of Boosting algorithm that integrates multiple decision trees to form a strong classifier. For a dataset with n samples and m features, the XGBoost model can be represented as the formula (8):

$$\hat{y}_i = \sum_{k=1}^{K} f_k(x_i), \quad f_k \in F \quad (i = 1, 2, \ldots, n) \tag{8}$$

The model aims to minimize the objective function, which is a sum of overall loss L and regularization term Ω.

$$\text{Obj} = L + \Omega \tag{9}$$

$$L = \sum_{i=1}^{n} (y_i - \hat{y}_i)^2 \tag{10}$$

$$\Omega = \gamma T + \frac{1}{2} \lambda \sum_{j=1}^{T} w_j^2 \tag{11}$$

Where γ is the regularization parameter for the number of leaves. λ is the regularization parameter for leaf weights. T and w_j denote the number of leaves and weight of leaf j in the tree, respectively.

F. Evaluation Strategy and Metrics

Each model was evaluated across 50 randomized trials, with the dataset partitioned into 80% for training and 20% for testing using stratified sampling. Additionally, stratified 5-fold cross-validation was implemented to optimize model parameters and reduce the risk of overfitting. To address the class imbalance, the Synthetic Minority Over-sampling Technique (SMOTE) was applied to the training set. SMOTE generates synthetic samples for the minority class by interpolating between existing minority class samples and their nearest neighbors, thus creating a more balanced dataset without simply duplicating data points.

Confusion Matrix (IV) is a table used in machine learning and statistics to evaluate the performance of classification models. It displays the classification results of the model in a matrix format, comparing the model's predictions with the actual labels.

TABLE IV CONFUSION MATRIX

Confusion Matrix		**Prediction**	
		Positive	**Negative**
Label	**Positive**	True positive (TP)	False positive (FP)
	Negative	False negative (FN)	True negative (TN)

$$\text{Accuracy} = \frac{TP + TN}{TP + TN + FP + FN} \tag{12}$$

$$\text{Recall} = \frac{TP}{TP + FN} \tag{13}$$

$$\text{Specificity} = \frac{TN}{TN + FP} \tag{14}$$

$$\text{Precision} = \frac{TP}{TP + FP} \tag{15}$$

$$\begin{aligned} \text{F1 score} &= 2 \times \frac{\text{Precision} \times \text{Recall}}{\text{Precision} + \text{Recall}} \\ &= \frac{2TP}{2TP + FP + FN} \end{aligned} \tag{16}$$

Among the evaluation metrics, accuracy represents the proportion of correctly classified results among all predictions; sensitivity/recall indicates the proportion of positive samples that are correctly identified; specificity refers to the proportion of negative samples that are correctly identified; F1 score is the weighted harmonic mean of precision and recall, providing a balanced measure that accounts for both false positives and false negatives. The area under the curve (AUC) measures the area under the receiver operating characteristic (ROC) curve. One notable property of ROC curves is their invariance to

changes in the distribution of positive and negative samples within the test set. The AUC value ranges from 0 to 1, where a value closer to 1 indicates that the model's classification performance closely aligns with the true labels. Conversely, an AUC value approaching 0.5 suggests that the model's predictions are akin to those of a random classifier, indicating no meaningful relationship between the features and the target variable.

IV. Results

A. Demographic Characteristics

We gathered data on demographic factors such as cardiovascular disease, use of antihypertensive medications, quitting smoking, stroke, use of walking aids, and history of falls. Then, we could evaluate the consistency of the various parameters to identify the significant difference between high-risk and low-risk fallers. Data analysis revealed significant differences between high-risk and low-risk groups in the following variables: "cardiovascular disease," "antihypertensive medication," "no smoking," "stroke," "use of walking aids," and "history of falls." Details are presented in Table V.

B. Visualization of Sensor Data

Figure 3 (a) and (b) show the 3-axis gyroscope data for one individual from each group during a segmented 3M-TUG task. Figures 3 (c) and (d) show that the high-risk faller had a lower range of motion, a less marked turn state, and a longer total 3M-TUG time than the low-risk faller. The angular velocity signal data for the turn phase were also compared, and a significant increase in the angular velocity of the turn was observed in low-risk fallers relative to high-risk fallers.

C. Significant Features

We employed the proposed sensor integration method to identify predictive indicators valuable for fall risk classification in the geriatric rehabilitation population. These significant features selected by Boruta include statistical metrics extracted from the IMU data: "Y-axis acceleration kurtosis," "Y-axis angular velocity variance," "Z-axis acceleration variance," "Y-axis angular velocity skewness," "X-axis angular velocity skewness," "Acceleration magnitude kurtosis," "Z-axis angular velocity mean," "Angular velocity magnitude kurtosis" and spatiotemporal parameters extracted from the Kinect data: "Total time," "Average stride length," "Speed," "Average step length," "Step count," "Turning curvature," "Average stride time," "Cadence". We also determined the optimal feature set after sensor integration through cross-validation, which includes "Total time," "Step count," "Y-axis acceleration kurtosis," and "Z-axis acceleration variance."

TABLE V THE SIGNIFICANT GENERAL CHARACTERISTIC OF THE PARTICIPANTS

Parameter	Low-risk fallers	High-risk fallers	p Value
Participants	30	26	-
Fall history (Y/N)	2/28	13/13	**
Gender (F/M)	14/16	6/20	0.066
Cardiovascular disease (Y/N)	10/20	19/7	0.003**
Osteoporosis (Y/N)	10/20	12/14	0.327
Antihypertensive medication (Y/N)	14/16	21/5	0.009**
Antihyperlipidemic drugs (Y/N)	9/21	7/19	0.799
Arthralgia (Y/N)	11/19	4/22	0.073
No smoking (Y/N)	24/6	13/13	0.018*
Stroke (Y/N)	11/19	17/9	0.032*
Usage of walking assistance (Y/N)	0/30	14/12	**

Note: $*p < 0.05$, $**p < 0.01$

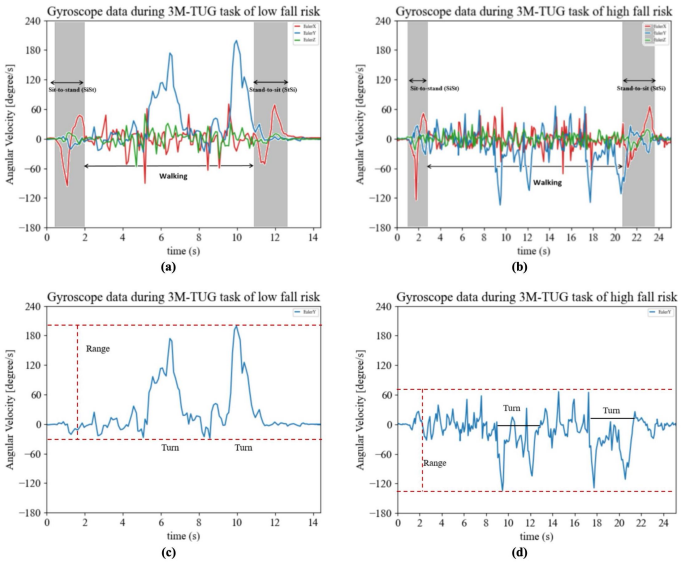

Fig. 3 Gyroscope Data During the 3M-TUG Task of Participants with Low and High Fall Risk.

To quantitatively delineate the disparities between the high-risk and low-risk groups, we employed the t-test or Mann-Whitney U test and the results are presented in Table VI and visually depicted in Figure 4.

D. Predictive Model Performance

The performance metrics of five predictive models on the test set are summarized in Table VII and visualized as ROC curves in Figure 5. The integrated feature set exhibited superior overall performance, with the model achieving an AUC ranging from 0.8633 to 0.9586, where KNN, SVM, LR performed the best. We hypothesize that there is significant gait heterogeneity among geriatric rehabilitation patients with different levels of fall risk, making it sufficient to classify them using only a few key features.

We also focused on the predictive performance of individual sensors to address scenarios where sensor integration may not be feasible in real-world environments. The results showed that models utilizing the Kinect feature set achieved an AUC ranging from 0.8538 to 0.9252, while the IMU feature set yielded an AUC between 0.8024 and 0.9267. Although these results were not as high as those achieved through sensor integration, the individual sensor still demonstrated excellent predictive capabilities, validating the practicality of the features we extracted. Therefore, we have reason to believe that

the proposed sensor integration method for geriatric rehabilitation patients can effectively identify individuals at high risk of falling, thereby reducing missed diagnoses and fall incidents.

V. Discussion

A. Complementary Contributions of Kinect and IMUs

Although the accuracy of IMUs and Kinect is considered acceptable compared to motion capture systems [36], single-sensor applications are often subject to various interferences. For instance, Kinect's depth sensing is highly sensitive to environmental factors including lighting and spatial positioning [24], [25], while IMUs are influenced by placement variability and sensor drift [27]. In rehabilitation settings, where geriatric patients with complex comorbidities are common, there is a critical need to improve evaluation accuracy to reduce the risk of adverse inpatient events. The integration of features from both sensors can help mitigate these limitations and reduce the impact of noise associated with individual sensors, thereby improving model robustness.

Kinect, with its skeletal recognition capabilities, provides significant advantages in detecting specific postures, including gait, turning, and sit-to-stand transitions [32], [33]. This technology captures critical transition moments with high accuracy. It facilitates the segmentation of the 3M-TUG test into distinct sub-task phases. It enables the measurement of key spatiotemporal gait parameters, such as gait speed, cycle time, stride length, minimum hip flexion angle, and maximum knee flexion angle [34]. While IMU-derived spatiotemporal gait parameters, such as stride length and step time, demonstrate acceptable accuracy, developing a high-precision stride estimation algorithm remains a significant challenge [37]. Hosseini et al. [38] demonstrated that IMUs can effectively capture fine-grained movements and perform well under extreme conditions. They provide detailed motion data that reflects the complexity of individual movement dynamics. This study found that anatomical parameters, such as joint angles during the 3M-TUG, lacked predictive value for falls. However, some studies suggest that certain features unique to Kinect skeletal data, which are not obtainable from IMUs, may exhibit specific advantages [30], [39].

Therefore, integrating Kinect and IMUs enhances the diversity of the feature set and improves adaptability to individual differences and varying gait patterns. This integration facilitates more accurate and personalized fall risk assessments for geriatric patients.

B. Feature Analysis and Implications for Fall Risk

Figure 6 shows the frequency of selected features extracted separately from IMU and Kinect. The color of the bars indicates the impact of each feature on fall risk, with the magnitude of the impact values presented in Table VIII.

Geriatric rehabilitation patients at high risk of falling tend to exhibit elevated kurtosis in both acceleration and angular velocity vectors. This observation suggests that these individuals may intentionally adopt slower movements during walking or turning to achieve greater movement consistency. However, they simultaneously experience gait instability or disruptions, leading to extreme acceleration and angular velocity fluctuations. Furthermore, these patients demonstrate reduced variance in Y-axis angular velocity and Z-axis acceleration, along with a lower mean Z-axis angular velocity, indicating restricted movement and diminished variability.

Such characteristics may reflect a rigid gait pattern and an underlying fear of falling, consistent with findings reported by Snijders [40] and Li [41]. Additionally, this study identified a distinct pattern in the high-risk group, where vertical angular velocity follows a left-skewed distribution, while lateral angular velocity follows a right-skewed distribution. This contrasts with the distribution patterns observed in the low-risk group, a phenomenon that remains underexplored in previous research.

Additionally, our findings suggest that individuals at high risk of falling exhibit longer completion times, average stride time [42], and take more steps [38]. These patterns are accompanied by lower walking speed, reduced cadence, and

TABLE VI SUMMARY OF KEY FEATURES IN THE 3M-TUG TASK

Features	Low-Risk Fallers Median (IQR)	High-Risk Fallers Median (IQR)	p-value
Y-axis acceleration kurtosis	0.7072 (0.2211, 1.0527)	2.5984 (1.6043, 3.9339)	$*$
Y-axis angular velocity variance	213.2938 (115.0687, 288.7203)	43.7937 (24.2277, 73.1538)	$***$
Z-axis acceleration variance	0.01427 (0.0080, 0.0252)	0.0043 (0.0031, 0.0089)	$*$
Y-axis angular velocity skewness	0.0384 (-0.2560 , 0.2716)	-0.3284 (-0.5972, -0.1776)	0.0025
X-axis angular velocity skewness	-0.3558 (-0.7581, -0.1599)	0.1682 (-0.1396, 0.7366)	0.0016
Acceleration magnitude kurtosis	1.2599(0.4804, 2.8255)	2.8439 (1.6387, 22.6802)	0.0038
Z-axis angular velocity mean	20.6236 (0.0058, 27.6736)	5.8746 (2.6986, 7.0402)	0.0236
Angular velocity magnitude kurtosis	1.0691 (0.2473, 1.7431)	2.1028 (1.0904, 3.5748)	0.0115
Total time	11.6667 (10.8417, 16.6167)	45.1833 (33.6500, 62.5250)	$***$
Average stride length	0.9509 (0.6887, 1.0981)	0.4432 (0.3526, 0.5216)	0.0279
Speed	1.2617 (0.8452, 1.4342)	0.3676 (0.2970, 0.5370)	$***$
Average step length	0.4279 (0.3523, 0.4994)	0.2118 (0.1838, 0.26258)	$***$
Step count	13 (11.0000, 15.2500)	25.0000 (22.7500, 28.2500)	$***$
Average turning curvature	4.2840 (2.8984, 16.8915)	76.1311 (32.0683, 179.4554)	$**$
Average stride time	1.2097 (1.14861, 1.3586)	2.1041 (1.3168, 2.6949)	$*$
Cadence	1.3343 (1.1620, 1.4242)	0.8454 (0.7343, 1.2261)	0.0010

Note: IQR = Interquartile Range; $*p < 0.001$; $**p < 0.0001$; $***p < 0.00001$.

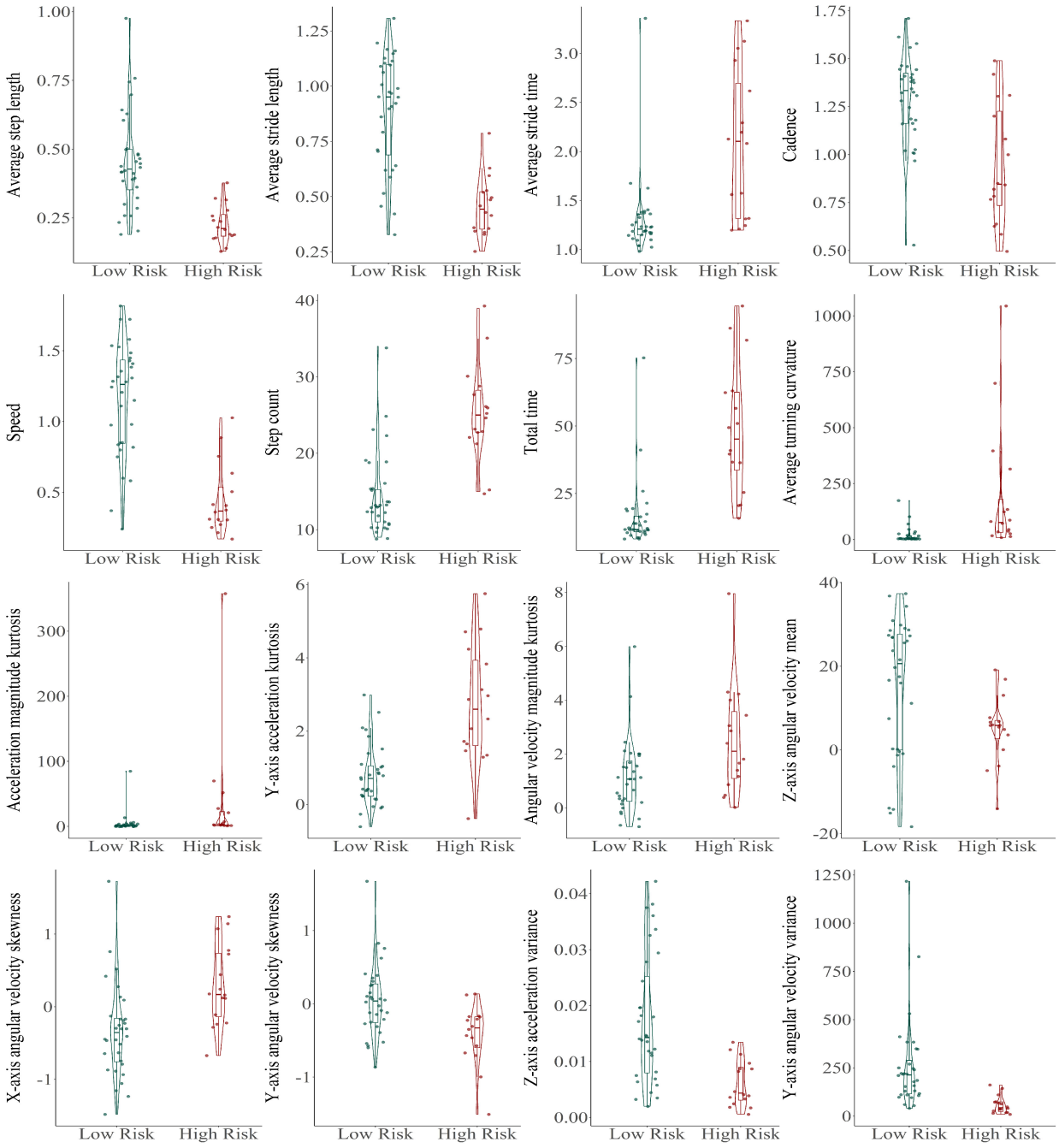

Fig. 4 Distribution of Spatiotemporal and IMU-Derived Features for Fall Risk Classification in Low-Risk and High-Risk Groups

shorter step and stride lengths [43], indicating decreased walking efficiency, potentially associated with restricted mobility. Furthermore, higher turning curvature [44] suggests that these individuals display irregular and discontinuous gait patterns during turning. These observations are consistent with findings in healthy geriatric populations [30], highlighting the capability of our integrated sensor system to efficiently identify potential fallers in rehabilitation settings.

The sensor integration method proposed in this study improves the interpretability of screening results, offering healthcare professionals, patients, and their families transparent and clear decision-making pathways.

C. Practicality and Performance of Integrated Sensors in Rehabilitation Setting

For geriatric patients undergoing rehabilitation, we aim to continuously assess fall risk throughout the recovery process. However, the complexity of the evaluation method may impact participants' willingness to engage and potentially affect its effectiveness. The IMU, as a portable sensor, is compact and lightweight, and when worn at the waist, it does not interfere with patients' daily activities. Meanwhile, the Kinect system uses a depth camera to capture human motion without requiring markers on the body surface, thereby improving pa-

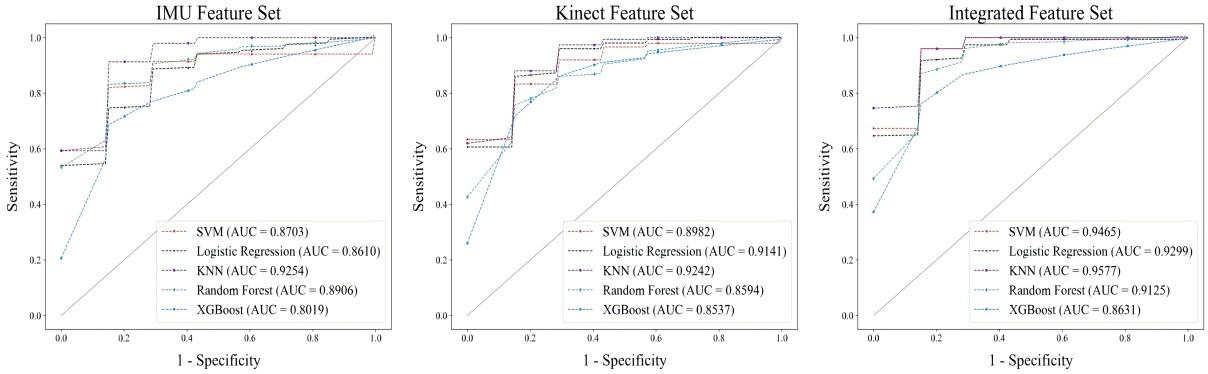

Fig. 5 ROC Curve of Different Models

TABLE VII PERFORMANCE METRICS OF DIFFERENT MODELS

Sensor	Model	Accuracy	Precision	Recall	F1	AUC
Kinect	SVM	0.8400	0.7153	0.8867	0.7764	0.9090
	LR	0.8180	0.6796	0.9067	0.7573	0.9152
	KNN	0.8340	0.7187	0.8467	0.7590	0.9252
	RF	0.7920	0.6774	0.7933	0.6957	0.8600
	XGBoost	0.8200	0.7162	0.7800	0.7166	0.8538
IMU	SVM	0.8680	0.7460	0.9533	0.8237	0.8200
	LR	0.7940	0.6389	0.8400	0.7025	0.8619
	KNN	0.8700	0.7482	0.9533	0.8259	0.9267
	RF	0.8420	0.7609	0.7867	0.7450	0.8914
	XGBoost	0.7860	0.6216	0.7067	0.6373	0.8024
Integrated Sensor	SVM	0.9240	0.8613	0.9267	0.8830	**0.9476**
	LR	0.8580	0.7680	0.8400	0.7817	**0.9301**
	KNN	0.9260	0.8790	0.9067	0.8831	**0.9586**
	RF	0.8640	0.7833	0.8267	0.7811	**0.9133**
	XGBoost	0.8320	0.7365	0.7333	0.7085	**0.8633**

tient compliance. As a result, the proposed sensor integration method demonstrates high acceptability among both patients and healthcare providers.

Our preliminary exploration of the gait analysis module within the integrated method highlights its ability to achieve excellent classification performance. Notably, this performance is attained using only four significant motion indicators: accuracy (0.9260), precision (0.8790), recall (0.9067), F1 score (0.8831), and AUC (0.9586). Importantly, this result is achieved without employing complex model integration methods or deep learning approaches. This finding is particularly important for clinical applications. Moreover, the integrated method enables effective classification using data from a single-source sensor. This demonstrates strong practicality in resource-limited scenarios. It is also effective when the data quality from one sensor is suboptimal.

A study using four classic machine learning models reported a mean accuracy of 75% for classifying both patients and healthy subjects using Kinect [31]. Another study on community-dwelling older adults demonstrated that combining IMU and Kinect features significantly improved fall risk assessment compared to single-sensor approaches, achieving an AUC of 88.2% [30]. In our study, we successfully validated the feasibility of sensor integration and machine learning models for fall risk prediction in real-world rehabilitation settings. This provides a new perspective for future research directions.

D. Discrepancy Between TUG Threshold and BBS

TUG completion time is widely used as a quick screening indicator for fall risk in both community and institutional settings [45], [46]. A threshold of 13.5 seconds has been shown to achieve 90% classification accuracy in community-dwelling older adults [47]. However, using McNemar's test, this study found that the 13.5-second criterion and the 40-point BBS threshold do not exhibit consistency in fall risk classification (Table IX, $\chi^2 = 14.67$, $p = 0.0001$, Cohen's Kappa = 0.53). This suggests that the 13.5-second threshold is not suitable for rehabilitation settings involving patients with complex comorbidities. Population heterogeneity and measurement bias further complicate the establishment of a strict cutoff value for identifying high fall risk individuals in geriatric rehabilitation patients [48].

In contrast, the classification results from our proposed interpretable machine learning model, using KNN as an example, showed significant consistency with the BBS classification results (Table X, $\chi^2 = 39.63$, $p < 0.0001$, Cohen's Kappa = 0.95). This makes it a viable alternative for large-scale implementation, potentially replacing the current gold standard. The screening method proposed in this study reduces the medical resource waste caused by false positives while providing personalized and interpretable results.

TABLE VIII EFFECTS OF DIFFERENT FEATURES ON FALL RISK

Feature	Effect	Feature	Effect
Total time	0.6766	Y-axis Acceleration Kurtosis	0.6345
Average stride Length	-0.6786	Y-axis Angular Velocity Variance	-0.4877
Speed	-0.6899	Z-axis Acceleration Variance	0.4440
Average step length	-0.5882	Y-axis Angular Velocity Skewness	-0.4411
Step count	0.6736	X-axis Angular Velocity Skewness	-0.4274
Average turning curvature	0.4490	Acceleration Magnitude Kurtosis	-0.3181
Average stride time	0.5623	Z-axis Angular Velocity Mean	0.2697
Cadence	-0.5265	Angular Velocity Magnitude Kurtosis	0.3784

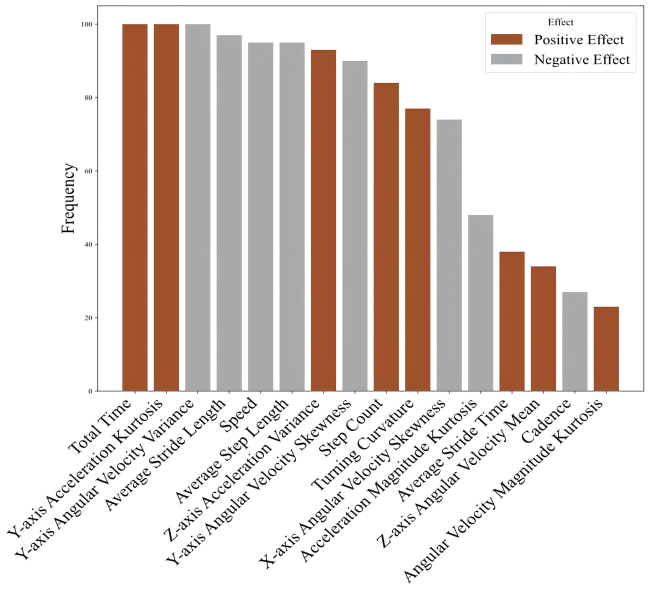

Fig. 6 Feature Frequency and Effect

TABLE IX CONTINGENCY TABLE ON BBS AND TUG TIME USING 13.5s CRITERIA

	BBS classifies as high fall risk (BBS score $\leq$ 40)	**BBS classifies as low fall risk (BBS score $>$ 40)**
TUG completion time classifies as high fall risk	16	12
TUG completion time classifies as low fall risk	0	20

TABLE X CONTINGENCY TABLE ON BBS AND TUG FEATURES USING KNN CLASSIFICATION

	BBS classifies as high fall risk (BBS score $\leq$ 40)	**BBS classifies as low fall risk (BBS score $>$ 40)**
KNN classified as high fall risk	16	1
KNN classified as low fall risk	0	31

REFERENCE

[1] National Quality Forum, "Serious reportable events. 2011 final report," https://www.qualityforum.org/topics/sres/serious_reportable_events.aspx, 2011, accessed May 10, 2022.

[2] J. Zhang, M. Wang, and Y. Liu, "Psychometric validation of the chinese version of the johns hopkins fall risk assessment tool for older chinese inpatients," *Journal of Clinical Nursing*, vol. 25, pp. 2846–2853, 2016.

[3] World Health Organization, "Rehabilitation," https://www.who.int/news-room/fact-sheets/detail/rehabilitation, 2024, retrieved November 26, 2024.

[4] Y. Y. et al., "Prevalence and risk factors of cerebral small vessel disease from a population-based cohort in china," *Neuroepidemiology*, vol. 57, no. 6, pp. 413–422, 2023.

[5] T. I. et al., "Osteosarcopenia, the co-existence of osteoporosis and sarcopenia, is associated with social frailty in older adults," *Aging Clinical and Experimental Research*, vol. 34, pp. 535–543, 2022.

[6] X. G. et al., "Current state and challenges of rehabilitation needs among elderly — china, 1990–2019," *China CDC Weekly*, vol. 4, no. 39, pp. 871–874, 2022.

[7] C. Stern and R. Jayasekara, "Interventions to reduce the incidence of falls in older adult patients in acute-care hospitals: a systematic review," *International Journal of Evidence-Based Healthcare*, vol. 7, pp. 243–249, 2009.

[8] S. V. et al., "Determinants influencing the implementation of multifactorial falls risk assessment and multidomain interventions in community-dwelling older people: a systematic review," *Age and Ageing*, vol. 53, no. 7, 2024.

[9] E. B. et al., "Is the timed up and go test a useful predictor of risk of falls in community-dwelling older adults: a systematic review and meta-analysis," *BMC Geriatrics*, vol. 14, p. 14, 2014.

[10] D. S. et al., "Discriminative ability and predictive validity of the timed up and go test in identifying older people who fall: systematic review and meta-analysis," *Journal of the American Geriatrics Society*, vol. 61, no. 2, pp. 202–208, 2013.

[11] O. B. et al., "Timed up and go test and risk of falls in older adults: A systematic review," *The Journal of Nutrition, Health and Aging*, vol. 15, no. 10, pp. 933–938, 2011.

[12] S. G. et al., "European consensus on core principles and future priorities for geriatric rehabilitation: consensus statement," *European Geriatric Medicine*, vol. 11, pp. 233–238, 2020.

[13] B. S. L. et al., "A classification and regression tree for predicting recurrent falling among community-dwelling seniors using home-care services," *Canadian Journal of Public Health*, vol. 100, pp. 263–267, 2009.

[14] M. G. et al., "Comparison of reliability, validity, and responsiveness of the mini-bestest and berg balance scale in patients with balance disorders," *Physical Therapy*, vol. 93, no. 2, pp. 158–167, 2013.

[15] S. L. W. et al., "Establishing the reliability and validity of measurements of walking time using the emory functional ambulation profile," *Physical Therapy*, vol. 79, no. 12, pp. 1122–1133, 1999.

[16] S. K. et al., "Validity of the community balance and mobility scale in community-dwelling persons after stroke," *Archives of Physical Medicine and Rehabilitation*, vol. 91, no. 6, pp. 890–896, 2010.

[17] A. M. et al., "A fall risk assessment mechanism for elderly people through muscle fatigue analysis on data from body area sensor network," *IEEE Sensors Journal*, vol. 21, no. 5, pp. 6679–6690, 2021.

[18] A. S. et al., "Quantitative assessment of balance impairment for fall-risk estimation using wearable triaxial accelerometer," *IEEE Sensors Journal*, vol. 17, no. 20, pp. 6743–6751, 2017.

[19] E. S. et al., "A comprehensive assessment of gait accelerometry signals in time, frequency and time-frequency domains," *IEEE Transactions on Neural Systems and Rehabilitation Engineering*, vol. 22, no. 3, pp. 603–612, 2014.

[20] T. Kim, X. Yu, and S. Xiong, "A multifactorial fall risk assessment system for older people utilizing a low-cost, markerless microsoft kinect," *Ergonomics*, pp. 1–19, 2023.

[21] J. Latorre, C. Colomer, M. Alcaniz, and R. Llorens, "Gait analysis with the kinect v2: Normative study with healthy individuals and comprehensive study of its sensitivity, validity, and reliability in individuals with stroke," *Journal of NeuroEngineering and Rehabilitation*, vol. 16, no. 1, pp. 1–11, 2019.

[22] A. H. B. et al., "Assessing the reliability and validity of inertial measurement units to measure three-dimensional spine and hip kinematics during clinical movement tasks," *Sensors*, vol. 24, no. 6580, 2024.

[23] J. A. Albert, V. Owolabi, A. Gebel, C. M. Brahms, U. Granacher, and B. Arnrich, "Evaluation of the pose tracking performance of the azure kinect and kinect v2 for gait analysis in comparison with a gold standard: A pilot study," *Sensors*, vol. 20, no. 5104, 2020.

[24] T. Mallick, P. P. Das, and A. K. Majumdar, "Characterizations of noise in kinect depth images: A review," *IEEE Sensors Journal*, vol. 14, no. 6, pp. 1731–1740, 2014.

[25] L. Yang, L. Zhang, H. Dong, A. Alelaiwi, and A. E. Saddik, "Evaluating and improving the depth accuracy of kinect for windows v2," *IEEE Sensors Journal*, vol. 15, no. 8, pp. 4275–4285, 2015.

[26] B. Galna, G. Barry, D. Jackson, D. Mhiripiri, P. Olivier, and L. Rochester, "Accuracy of the microsoft kinect sensor for measuring movement in people with parkinson's disease," *Gait Posture*, vol. 39, no. 4, pp. 1062–1068, 2014.

[27] Y.-S. C. et al., "Evaluation of validity and reliability of inertial measurement unit-based gait analysis systems," *Annals of Rehabilitation Medicine*, vol. 42, no. 6, pp. 872–883, 2018.

[28] R. Sun and J. J. Sosnoff, "Novel sensing technology in fall risk assessment in older adults: A systematic review," *BMC Geriatrics*, vol. 18, pp. 1–10, 2018.

[29] M. Kepski and B. Kwolek, "Event-driven system for fall detection using body-worn accelerometer and depth sensor," *IET Computer Vision*, vol. 12, no. 1, pp. 48–58, 2017.

[30] X. Wang, J. Cao, and Q. Zhao, "Identifying sensors-based parameters associated with fall risk in community-dwelling older adults: An investigation and interpretation of discriminatory parameters," *BMC Geriatrics*, vol. 24, p. 125, 2024.

[31] S. R. Tripathy, K. Chakravarty, and A. Sinha, "Eigen posture based fall risk assessment system using kinect," in *Proc. IEEE Int. Conf. Eng. Med. Biol. Soc. (EMBC)*, 2018, pp. 1–4.

[32] Y. Wang, J. Sun, J. Li, and D. Zhao, "Gait recognition based on 3d skeleton joints captured by kinect," in *Proc. IEEE Int. Conf. Image Process. (ICIP)*, 2016, pp. 3151–3155.

[33] E. Acorn, N. Dipsis, T. Pincus, and K. Stathis, "Sit-to-stand movement recognition using kinect," in *Statistical Learning and Data Sciences. SLDS 2015. Lecture Notes in Computer Science*, vol. 9047. Springer, Cham, 2015.

[34] J. Latorre, C. Colomer, and M. Alcañiz, "Gait analysis with the kinect v2: Normative study with healthy individuals and comprehensive study of its sensitivity, validity, and reliability in individuals with stroke," *Journal of NeuroEngineering and Rehabilitation*, vol. 16, p. 97, 2019.

[35] C.-Y. Sun, L.-C. Hsu, and C.-C. Su, "Gait abnormalities and longitudinal fall risk in older patients with end-stage kidney disease and sarcopenia," *BMC Geriatrics*, vol. 24, p. 937, 2024.

[36] P. Jatesiktat, D. Anopas, and W. T. Ang, "Personalized markerless upper-body tracking with a depth camera and wrist-worn inertial measurement units," in *Proc. IEEE Eng. Med. Biol. Soc. (EMBC)*, 2018, pp. 1–6.

[37] D. Trojaniello, A. Cereatti, and U. D. Croce, "Accuracy, sensitivity and robustness of five different methods for the estimation of gait temporal parameters using a single inertial sensor mounted on the lower trunk," *Gait Posture*, vol. 40, no. 4, pp. 487–492, 2014.

[38] I. Hosseini, R. F. Rojas, and M. Ghahramani, "Fall risk assessment using single imu," in *Proc. IEEE Int. Symp. Med. Meas. Appl. (MeMeA)*, 2024, pp. 1–6.

[39] D. Webster and O. Celik, "Systematic review of kinect applications in elderly care and stroke rehabilitation," *Journal of NeuroEngineering and Rehabilitation*, vol. 11, p. 108, 2014.

[40] A. H. Snijders, B. P. van de Warrenburg, N. Giladi, and B. R. Bloem, "Neurological gait disorders in elderly people: Clinical approach and classification," *Lancet Neurology*, vol. 6, no. 1, pp. 63–74, 2007.

[41] F. Li, K. J. Fisher, P. Harmer, E. McAuley, and N. L. Wilson, "Fear of falling in elderly persons: Association with falls, functional ability, and quality of life," *The Journals of Gerontology: Series B*, vol. 58, no. 5, pp. P283–P290, 2003.

[42] F. B. et al., "Timed up and go and six-minute walking tests with wearable inertial sensor: One step further for the prediction of the risk of fall in elderly nursing home people," *Sensors*, vol. 20, no. 11, p. 3207, 2020.

[43] Y. D. et al., "A novel environment-adaptive timed up and go test system for fall risk assessment with wearable inertial sensors," *IEEE Sensors Journal*, vol. 21, no. 16, pp. 18 287–18 297, 2021.

[44] J. M. Leach, S. Mellone, and P. Palumbo, "Natural turn measures predict recurrent falls in community-dwelling older adults: A longitudinal cohort study," *Scientific Reports*, vol. 8, p. 4316, 2018.

[45] D. Podsiadlo and S. Richardson, "The timed 'up go': A test of basic functional mobility for frail elderly persons," *Journal of the American Geriatrics Society*, vol. 39, pp. 142–148, 1991.

[46] H. A. B. et al., "Identifying a cut-off point for normal mobility: A comparison of the timed 'up and go' test in community-dwelling and institutionalised elderly women," *Age and Ageing*, vol. 32, no. 3, pp. 315–320, 2003.

[47] A. Shumway-Cook, S. Brauer, and M. Woollacott, "Predicting the probability for falls in community-dwelling older adults using the timed up go test," *Physical Therapy*, vol. 80, no. 9, pp. 896–903, 2000.

[48] D. Podsiadlo and S. Richardson, "The timed 'up go': A test of basic functional mobility for frail elderly persons," *Journal of the American Geriatrics Society*, vol. 39, pp. 142–148, 1991.